A massive phytoplankton bloom induced by an ecosystem-scale iron fertilization experiment in the equatorial Pacific Ocean

Kenneth H. Coale*, Kenneth S. Johnson*†, Steve E. Fitzwater*, R. Michael Gordon*, Sara Tanner*, Francisco P. Chavez†, Laurie Ferioli*†, Carole Sakamoto†, Paul Rogers†, Frank Millero‡, Paul Steinberg‡, Phil Nightingale§||, David Cooper§||, William P. Cochlan¶, Michael R. Landry#, John Constantinou#, Gretchen Rollwagen#, Armando Trasvina☆|| & Raphael Kudela¶||

* Moss Landing Marine Laboratories, PO Box 450, Moss Landing, California 95039-0450, USA
† Monterey Bay Aquarium Research Institute, PO Box 628, Moss Landing, California 95039-0628, USA
‡ University of Miami, 4600 Rickenbacker Causeway, Key Biscayne, Florida 33149, USA
§ School of Environmental Sciences, University of East Anglia, Norwich NR4 7TJ, UK
¶ Hancock Institute for Marine Studies, University of Southern California, Los Angeles, California 90089-0371, USA
# Department of Oceanography, University of Hawaii at Manoa, 1000 Pope Road, Honolulu, Hawaii 96822, USA
☆ CICESE Oceanografia Fisica, Km 107 Carret. Tijuana-Ensenada, Ensenada, B. C. Mexico

The seeding of an expanse of surface waters in the equatorial Pacific Ocean with low concentrations of dissolved iron triggered a massive phytoplankton bloom which consumed large quantities of carbon dioxide and nitrate that these microscopic plants cannot fully utilize under natural conditions. These and other observations provide unequivocal support for the hypothesis that phytoplankton growth in this oceanic region is limited by iron bioavailability.

THE persistence of high-nitrate, low-chlorophyll (HNLC) conditions in the surface waters of several large regions of the world's oceans comprise a familiar enigma in oceanography[1]. The factors that prevent the utilization of nitrate also regulate the rate at which carbon dioxide is taken up by phytoplankton and, ultimately, the amount of carbon exported from the surface waters. The oceans are both a major source and sink for atmospheric carbon dioxide, and processes that control the balance of these fluxes are thought to have a major effect on global climate[2]. Understanding the factors that limit the uptake of excess plant nutrients is, therefore, a key to understanding climate change. Grazing pressure exerted on phytoplankton by rapidly reproducing microzooplankton and micronutrient (iron) deficiency may function jointly in these HNLC waters[3]; yet the relative importance of each of these factors in controlling the biomass and rates of phytoplankton production has remained contentious[4]. The experimental tools available to the oceanographer have, until recently, been inadequate to resolve the relative importance of these processes. *In vitro* enrichment experiments[5–12], where iron is added at nanomolar levels to samples of sea water, invariably do not represent the *in situ* phytoplankton grazer community. The interpretation of such experiments has, therefore, been ambiguous to some[13–15].

In 1993, the first open-ocean iron enrichment experiment (IronEx I) was performed in an attempt to eliminate the ambiguity of *in vitro* containment and allow the processes influencing community structure and carbon export to operate at an appropriate scale[16]. IronEx I involved a single 4 nM enrichment of dissolved iron to an experimental 'patch' of equatorial Pacific surface waters[16]. This experiment demonstrated a clear and unambiguous physiological response to the addition of iron which resulted in a doubling of plant biomass, a tripling of chlorophyll concentrations and a fourfold increase in phytoplankton productivity. Four days after the iron addition, the patch was subducted beneath a layer of less-dense surface water; hence , the magnitude of the biological and geochemical response was much smaller than predicted from previous bottle enrichment experiments[5–12]. Nitrate drawdown during IronEx I was undetectable (<0.2 μM), and carbon dioxide fugacity was only reduced by 10 μatm (ref. 17).

Several hypotheses were advanced to explain this small biogeochemical response. (1) Iron was rapidly lost from the patch[16], (2) the subduction of the patch to lower light levels minimized the photodissolution of iron colloids and decreased rates of bioavailable iron production[18], (3) zooplankton quickly cropped the increase in phytoplankton biomass[16,19], and (4) another nutrient, such as zinc or silicate, became limiting thus preventing further growth[16,20]. The second mesoscale iron enrichment experiment (IronEx II) was designed to test these hypotheses. Multiple additions of iron, over several days, were used to simulate a natural iron input event, and zooplankton grazing rates and concentrations of other potentially limiting nutrients were closely monitored over the course of the experiment. The massive phytoplankton bloom triggered by the relief of iron-limitation was not significantly checked by either grazing or secondary nutrient limitation, thus unequivocally supporting the hypothesis

|| Present addresses: Plymouth Marine Laboratory, Prospect Place, West Hoe, Plymouth PL1 3DH, UK (P.N.); Department of Atmospheric and Oceanic Sciences, University of Wisconsin, 1225, West Dayton Street, Madison, Wisconsin 53706, USA (D.C.); Monterey Bay Aquarium Research Institute, PO Box 628, Moss Landing, California 95039-0628, USA (R.K.), Departamento de Oceanografia Fisica, Oceanografia Tropical, CICESE subsede Baja California Sur, Miraflores No. 334 entre Mulege y La Paz, Fracc. Bella Vista, La Paz 23050, B.C.S., Mexico (A.T.).

that the HNLC condition of these waters is due to iron-limitation of algal growth.

Experimental strategy

The IronEx II experiment involved three separate mesoscale infusions (patches 1, 2 and 3) and a series of deckboard *in vitro* enrichment experiments. A 1,000 km^2 area was surveyed in the vicinity of 3.5° S, 104° W in May 1995 to ensure that hydrographic, biological and chemical conditions were uniform throughout the region, to minimize the chance of surface-water subduction which biased the first iron enrichment experiment, and to ensure that changes in the experimental area could be attributed to the presence of iron.

Many of the experimental methodologies originally developed during IronEx I[16] were employed in the IronEx II experiment. All navigation was conducted relative to a central buoy, fixed within the mixed layer of the patch using a 1 × 20 m holey-sock drogue, that was set at a depth of 15 m. This buoy, instrumented with a global positioning system, packet radio, fluorometer, transmissometer, conductivity, oxygen and temperature sensors, served as the centre of a lagrangian frame of reference. The position of the buoy was transmitted to the ship every 5 min. Iron infusions and sampling transects were performed relative to this lagrangian buoy. The buoy drifted at about 2.8 km h^{-1} in a south-by-southwesterly direction over the duration of the experiment. A second instrumented buoy was deployed outside the iron-enriched area to monitor changes in the unperturbed waters. The central buoy was recovered 19 days after deployment, some 1,500 km from its initial position (Fig. 1).

On 29 May (day 0 of the patch 1 experiment), 225 kg of iron (as acidic iron sulphate) was mixed in constant ratio with the inert chemical tracer sulphur hexafluoride (SF_6) and then injected immediately aft of the ship's twin propellers as the ship steamed over a 72 km^2 rectangular deployment grid. Acidic iron sulphate is the form of iron thought most likely to enter the surface waters naturally through atmospheric deposition[21]. Based on a turbulent dispersion model[22], the iron streaks laid 400 m apart in the ship's track were calculated to merge within one day, resulting in a uniform addition of iron throughout the 25-m mixed layer. This uniformity was confirmed by both underway measurements and vertical profiles of SF_6 and Fe. Mixed-layer depth averaged 25 m during the infusion, and the initial (day 1) concentration was 2 nM Fe. Two subsequent infusions each of 112 kg of Fe (to yield an increase of 1 nM each) were performed on days 3 and 7 of the experiment to maintain an enhanced concentration of iron in patch 1. All infusions were performed using even track spacing. Subsequent surveys were both rectilinear and star-shaped.

A suite of hydrographic and biological measurements (temperature, salinity, Fe, SF_6, CO_2, dimethyl sulphide and its algal precursor, nutrients, primary productivity, trace elements, plant pigments including chlorophyll, grazing pressure, phytoplankton, zooplankton and heterotrophic bacterial abundances, isotopes (^{16}O, ^{18}O, ^{12}C, ^{13}C, ^{234}Th), colloids and metal speciation) were performed each day at vertical profile stations both inside and outside the experimental patch. Many of these data we report here, and in companion papers in this issue, and others will be reported elsewhere. 'Inside' stations were defined both by their

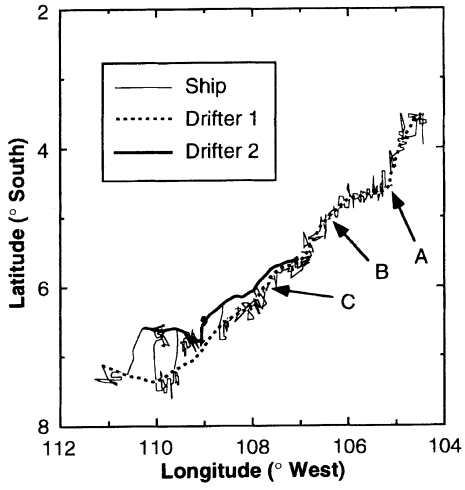

FIG. 1 The drift tracks of the lagrangian drifter buoys, indicating the centre of the enriched area, are plotted together with the ship's position during the IronEx II experiment. The dashed line indicates the track of the central lagrangian drifter buoy (drifter 1) marking the centre of patch 1 (sequentially infused). The thick solid line indicates the track of the central lagrangian drifter buoy (drifter 2) marking the midpoint between patch 2 (control; no iron addition) and patch 3 (+0.3 nM Fe). The thin line indicates the ship's track as it navigated about both buoys during the 19 days of the experiment. Initial patch 1 advection velocity (as determined by buoy 1) was close to 3 km h^{-1} requiring constant corrections to the lagrangian coordinate system. Buoy positions were transmitted to the ship every 5 min and were used to continuously update the navigational frame of reference. Arrows A, B and C designate the location of the initial 2 nM, and subsequent 1 nM, Fe infusions of patch 1, respectively. The drift track of the outside buoy is not shown.

FIG. 2 A series of contours of six measured variables plotted as a daily time series over the duration of the patch 1 experiment. These plots were constructed using Systat (statistical software from Systat, Inc., Evanston, IL, USA) with the data available from vertical profiles, underway sensors and discrete mixed-layer samples. The underway data was obtained using the ship's PVC pumping system which had an intake on the bow, ~6 m below the surface. On day 17, at the southwesternmost extent of the patch 1 experiment, a water mass of lower density and lower nutrients was encountered. The approximate location of this abutting water mass is depicted as a grey area in plots *b–f* on day 17. *a*, Vertical section of temperature along the drift track of buoy 1 (ordinate, depth in metres). This figure was constructed from vertical temperature profiles taken in or near patch 1 using a profiling conductivity–temperature–depth sensor deployed from the ship. It is constructed from discrete casts taken at various time intervals throughout the experiments and, therefore, does not represent a continuous trend in the temperature structure. Nonetheless, the general features of the thermocline can be seen from this plot. *b*, Areal contours of SF_6 concentrations in patch 1 over the course of the experiment. SF_6 was used as an inert chemical tracer marking the infused area and provided indication of the enriched waters after iron had been removed. Initial concentrations decreased rapidly due to outgassing to the atmosphere and mixing both vertically and horizontally. Tracer mixed below the thermocline was lost due to differential advection of the surface layer. Measurements of SF_6 were made using detection methodology described previously[15]. The gaps in the data on days 10–13, 15–16 represent times when the ship was at patch 2 and 3. The N.D. (not determined) for day 17 indicates that no underway determinations were made that day. *c*, Daily areal plots of iron concentration contoured over the course of the experiment. Underway measurements of iron were made using flow injection analysis with chemiluminescence detection[44] further modified for analysis at sea. Owing to the contamination near the ship, the ship's pumping system and the short sample load-times required for high spatial resolution mapping, the detection limit of the combined system was ~0.2 nM. Background values of ~0.02 nM dissolved iron were confirmed by electrochemical (E. Rue, personal communication) and modified atomic absorption methods[45]. These concentrations were encountered outside patch 1 and within patch 1 after day 9. *d*, Chlorophyll contour plots were generated using a flow-through fluorometer and calibrated with filtered chlorophyll samples extracted in acetone for 24 h at −20 °C and read on a calibrated fluorometer. The N.D. on day 7 indicates that no determinations were performed through the ship's pumping system on this day. *e*, Nitrate contours were constructed from measurements made while underway from the ship's flow-through system using an Alpkem segmented flow autoanalyser. The continuous nitrate record was calibrated with periodic standards and a daily series of discrete samples and standards run on an independent analyser. *f*, Areal contours of CO_2 fugacity (f_{CO_2}) were determined using a flowing system in which the water at 6-m depth, and air-equilibrated samples were measured with a LICOR non-dispersive infrared detector. The accuracy of the system was determined during the cruise with two standard gases (277.05 and 501.73 p.p.m. standards) that were measured every two hours.

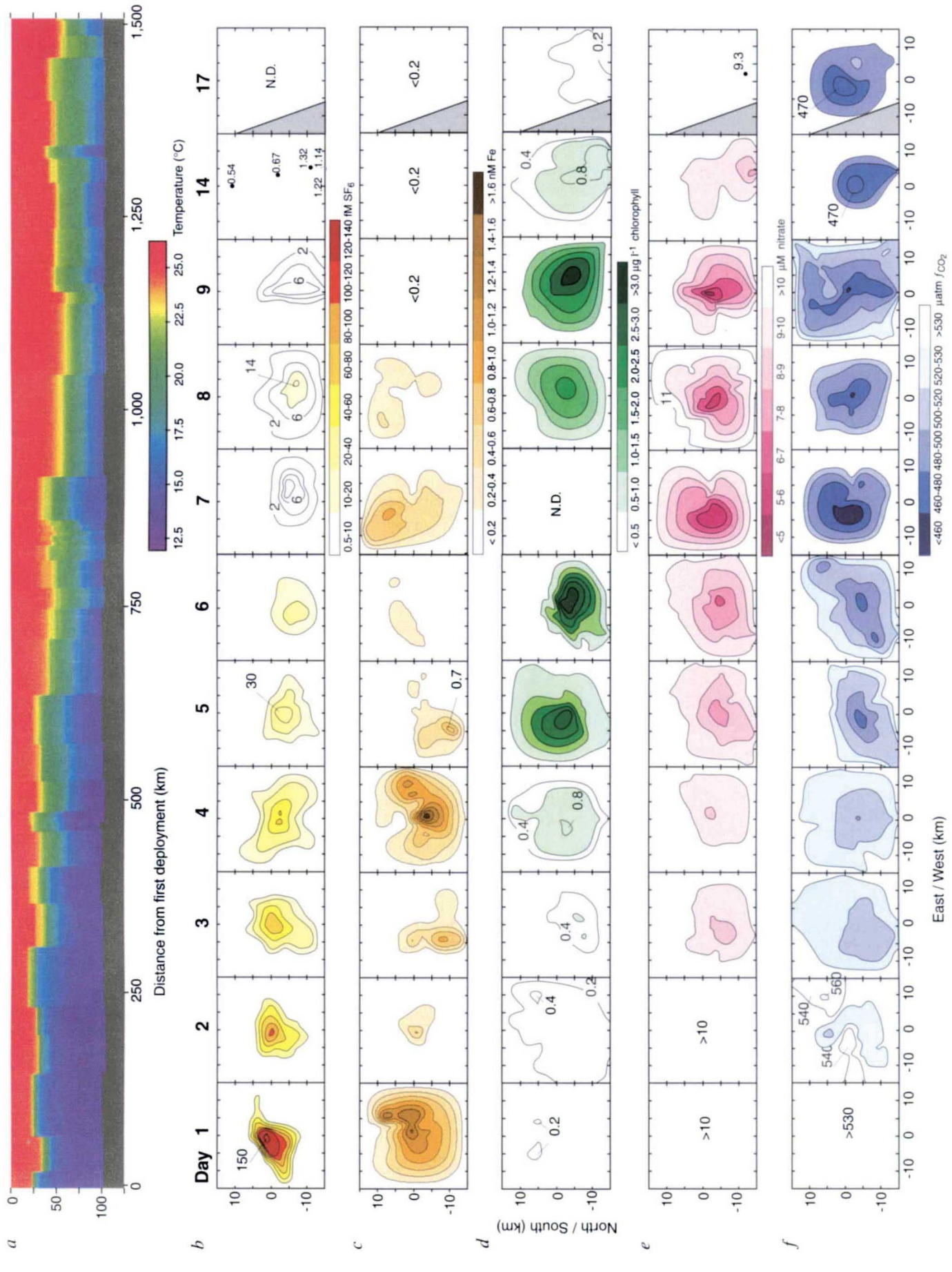
a
b
c
d
e
f
Day 1
2
3
4
5
6
7
8
9
14
17
Distance from first deployment (km)
Temperature (°C)
12.5 15.0 17.5 20.0 22.5 25.0
0.5-10 10-20 20-40 40-60 60-80 80-100 100-120 120-140 fM SF6
< 0.2 0.2-0.4 0.4-0.6 0.6-0.8 0.8-1.0 1.0-1.2 1.2-1.4 1.4-1.6 >1.6 nM Fe
< 0.5 0.5-1.0 1.0-1.5 1.5-2.0 2.0-2.5 2.5-3.0 >3.0 µg l-1 chlorophyll
<5 5-6 6-7 7-8 8-9 9-10 >10 µM nitrate
<460 460-480 480-500 500-520 520-530 >530 µatm fCO2
N.D.
North / South (km)
East / West (km)

proximity to the central buoy and by the SF_6 concentration. 'Outside' stations were located at areas with background levels of SF_6 and were generally near the outside buoy. Underway surveys using the ship's pumping system were conducted daily between inside and outside stations. The trends described here are based on measurements taken within the mixed layer at the daily inside stations. The seawater intake used for underway measurements was located on the bow at a depth of 6 m and therefore represents the water of the upper mixed layer.

Two smaller (24 km^2) patches were also created. One (patch 2) was infused with acidified sea water and SF_6, but no iron. This patch served as a control to test for possible effects due to transient acidification and the presence of the research vessel. The other (patch 3) received a single, low-level addition of iron (to 0.3 nM) plus SF_6. Patch 3 was created to mimic the concentration of iron associated with the equatorial undercurrent which upwells into surface-waters to the west of the study area[23].

Patch behaviour

Patch coherence was essential to the success of the experiment. The mixed layer deepened in a series of small mixing events from 25 m on day 1 to about 50 m by day 11 (Fig. 2*a*). As the mixed layer deepened, patch 1 mixed with higher-nutrient waters directly below. This was evident in periodic increases in nitrate concentrations within patch 1 and a deepening of the thermocline and SF_6 signal over time. Contours of SF_6 concentrations measured in the surface waters over the course of the experiment (Fig. 2*b*) indicated that patch 1 was fairly cohesive and expanded with time from an initial area of approximately 72 km^2 to over 120 km^2 by day 17. As the residence time of iron in these waters was short (see below) and the buoy slipped somewhat relative to the mixed layer owing to wind drift, SF_6 was used as the primary indicator to track the area enriched with iron and to distinguish 'inside' from 'outside' stations.

Rapid uptake/removal of the iron was observed following each of the iron infusions on days 0, 3 and 7 (Fig. 2*c*). As the biomass of patch 1 increased in response to added iron, the rate of iron removal also increased. Discrete iron analyses of mixed-layer samples indicated that iron concentrations decreased to below ambient levels (<0.02 nM) within three days following the last iron addition, (E. Rue and R.M.G., unpublished data) (Fig. 2*c*).

Biological and geochemical responses

Fluorescence measurements in patch 1 showed a rapid and monotonic increase in chlorophyll-*a* concentrations from an initial value of 0.15–0.20 $\mu g\,l^{-1}$ to values approaching 4 $\mu g\,l^{-1}$ on day 9, two days after the last infusion of iron (day 7). Maximum chlorophyll-*a* concentrations in patch 1 were 27 times the mean of initial and outside chlorophyll-*a* concentrations. Chlorophyll-*a* concentrations then decreased throughout the rest of the experiment, reaching 0.30 $\mu g\,l^{-1}$ on day 17 (Fig. 2*d*). Increased chlorophyll concentrations were found throughout the mixed layer in the patch (Fig. 3*b*).

The phytoplankton chlorophyll in patch 3 (+0.3 nM Fe) also showed a distinctive response to iron, increasing from 0.22 to 0.44 $\mu g\,l^{-1}$ after two days. The response of patch 3 is consistent with incubation experiments indicating a Michaelis–Menten relationship between dissolved iron concentration and community growth rates[23]. Given a half saturation constant of 0.12 nM (ref. 23), the addition of 0.3 nM iron should produce a two-fold change in community growth rate. The threshold for community response to iron addition is clearly at the sub-nanomolar level. No biological response was detected in the control patch which received only acidified sea water and the inert tracer SF_6. From this, we conclude that the observed community responses in patches 1 and 3 were due to the iron added and not to other chemicals or the presence of the ship. The remainder of this discussion will focus on the results of patch 1.

Nutrients were measured both continuously through the ship's seawater system, and in all discrete samples. Contour plots of

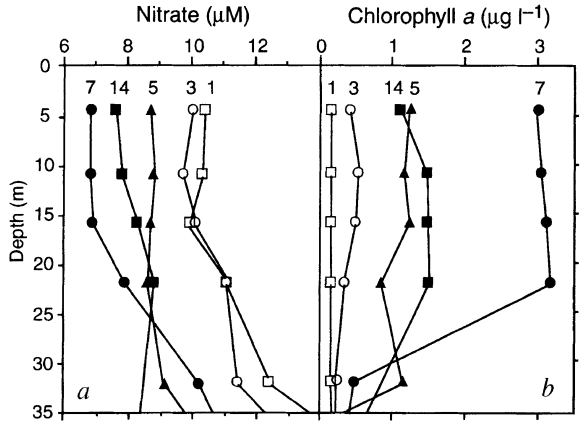

FIG. 3 *a*, Vertical profiles of mixed-layer nitrate from the daily 'inside-patch' stations of patch 1. Numbers at the top of each profile indicate the day of the patch 1 experiment. These plots illustrate the depletion of nitrate as the bloom reached its peak near days 7–9. The subsequent increase (day 14) is thought to be the result of mixing. Nitrate concentrations both inside and outside the patch converged to about 10 μM by ~50 m. *b*, As *a* but for mixed-layer chlorophyll *a*.

nitrate concentrations in surface waters throughout the experiment (Fig. 2*e*), as well as nitrate profiles at inside-patch stations (Fig. 3*a*), indicated a strong drawdown of approximately 5 μM nitrate as the biological response developed. Some nitrate may have been added by mixing from below as the mixed layer deepened (days 11, 14; Fig. 2*a*). Following an initial lag of one–two days, nitrate drawdown tracked silicate drawdown on an equimolar basis, suggesting that diatom growth was responsible for most of the nitrate uptake.

Rates of nitrate uptake by the planktonic assemblages were determined using the ^{15}N-isotope tracer technique[24]. Samples were collected using trace-metal-clean techniques[25] inside and outside (controls) of patch 1 from 15 m depth (~40% of the photon flux at 0.5 m) and incubated for ~6 h in Plexiglass incubators under simulated *in situ* light and temperature conditions. Absolute (transport) uptake rates of nitrate increased dramatically (14-fold increase) as a result of Fe enrichment, from <10 $nM\,h^{-1}$ (range 8.7–9.6 $nM\,h^{-1}$ in control and pre-fertilization samples) to a maximum rate of 133 $nM\,h^{-1}$ on day 6. Addition of Fe also increased biomass-specific rates of NO_3^- uptake by a factor of 5–7 by days 6 and 8, before declining to pre-fertilization rates. However, there was no discernible increase in particulate-nitrogen-specific uptake rates for the first 4 days after iron enrichment. The subsequent increase in particulate-nitrogen-specific uptake at the height of the iron-induced bloom is the result of faster rates of NO_3^- consumption per unit phytoplankton biomass, a result similar to that reported for iron amended bottle experiments in the equatorial Pacific near 140° W (refs 3, 10). Post-incubation size-fractionation of $^{15}NO_3^-$ accumulation (from parallel filtrations on Whatman GF/F filters and Poretics 5.0 μm silver membrane filters) demonstrated clearly that the large phytoplankton (>5.0 μm size fraction) were responsible for the enhanced NO_3^- utilization caused by Fe enrichment. The uptake by the >5.0 μm size fraction, which accounted for <15% of the total uptake before fertilization, increased to 85–98% of the total NO_3^- uptake at the peak of the phytoplankton bloom (days 6 and 8).

The carbon dioxide fugacity (f_{CO_2}) calculated from continuous CO_2 measurements of CO_2 partial pressure (p_{CO_2}) on board the ship, showed significant depletions within patch 1 which paralleled the drawdown of nitrate (Fig. 2*e*). The maximum depletion in f_{CO_2} was observed on day 9, coincident with the maximum in most other biological and chemical indicators of growth. The south equatorial Pacific at 105° W is a strong source of CO_2 to the

atmosphere (f_{CO_2} in seawater, 526 p.p.m.; f_{CO_2} in the atmosphere, 360 p.p.m.) (Fig. 2*f*). Iron-enhanced growth resulted in a drawdown of about 90 μatm, which strongly reduced outgassing of CO_2 from these waters. In spite of this drawdown, levels of CO_2 were at or above atmospheric partial pressure, and we do not believe the system became carbon-limited. The lack of limitation by carbon (or other micronutrients such as zinc) was supported by bottle enrichment experiments which consumed all available nitrate (see below).

Community response

To examine the community response to iron addition, the taxonomic composition of the plankton was determined using epifluorescence microscopy. Taxa-specific cell volumes and densities, converted to carbon using known carbon:volume relationships[26,27], indicated that biomass increased in all phytoplankton groups (Fig. 4*a*,*b*). Diatoms clearly showed the greatest increase in biomass over ambient (85×). The smaller organisms were less affected, with *Synechococcus* (1 μm) and red fluorescing picoplankton (<2 μm) only doubling in biomass. The biomass of microzooplankton (<200 μm), primarily small ciliates and flagellates, increased in step with the smaller autotrophs (2× increase). Mesozooplankton biomass (zooplankton >200 μm in length), comprised mainly of calanoid and cyclopoid copepods, also increased in patch 1 from 3.8 mg C m^{-3} measured from plankton net tows at control sites to 6.1 mg C m^{-3} in the patch. The highest mixed-layer concentration of mesozooplankton, 14 mg C m^{-3}, occurred in a daytime sampling of patch 1 on day 6.

Experimental dilution incubations[28] were performed to estimate both growth rates and grazing pressure on the small (<5 μm) phytoplankton that normally dominate the equatorial Pacific upwelling system[29–31] abundance. Phytoplankton abundance increased dramatically in patch 1 because they were able to grow faster, as a group, than the rates at which their consumers could remove them. Based on analyses of chlorophyll *a* in dilution incubations[28], the specific growth rate of the phytoplankton community averaged 1.25 d^{-1}, almost two cell divisions per day, during days 4-8. This was more than double the growth rate in ambient control waters, leaving a large imbalance between growth and grazing processes in the early phase of the plankton bloom response to added iron. Microzooplankton grazing rate averaged 0.32 d^{-1} (range of 0.17–0.48 d^{-1}) at control sites out of the patch, but increased by more than three times in the patch to 1.1 d^{-1} on day 7, as chlorophyll was reaching its peak concentration. The modest increase in patch densities of picoplankton (for example, *Synechococcus* spp. and small fluorescing picoplankton) during the experiments indicates that the increase in microzooplankton grazing was almost sufficient to keep the smaller members of the phytoplankton community in check[13,32]. In contrast, diatoms were clearly not contained by grazing, presumably because they were too large to be effectively consumed by the fast-growing microzooplankton, and too fast-growing to be suppressed by the larger mesozooplankton which have longer generation times with respect to the doubling rates of diatoms. This imbalance between production and grazing is analogous to the spring bloom of the North Atlantic[33].

The mesozooplankton grazing impact on phytoplankton, as deduced from analyses of gut pigment contents, was always small relative to that of the microzooplankton. The amount of phytoplankton pigment processed, per unit biomass of mesozooplankton, increased more or less in proportion to the increase in chlorophyll in patch 1. The community grazing effect of larger animals increased by about 50%, from 7.8% of phytoplankton standing stock per day at control sites to 11.4% d^{-1} in the patch, approximately in proportion to their increase in biomass. At the mixed-layer temperature of equatorial waters, the expected generation time of pelagic copepods of less than a week[34] could have allowed a more dramatic numerical response of the mesozooplankton to the bloom conditions. The lack of a stronger response could mean that these copepods are already growing at rapid rates in equatorial waters with high compensating rates of mortality due to predation.

Carbon removal

Measurements of both particulate and dissolved organic carbon (POC and DOC) concentrations throughout the experiments showed an increase in these two carbon pools. POC increased from 4 to 15 μM C at day 6 in patch 1. The increase in living

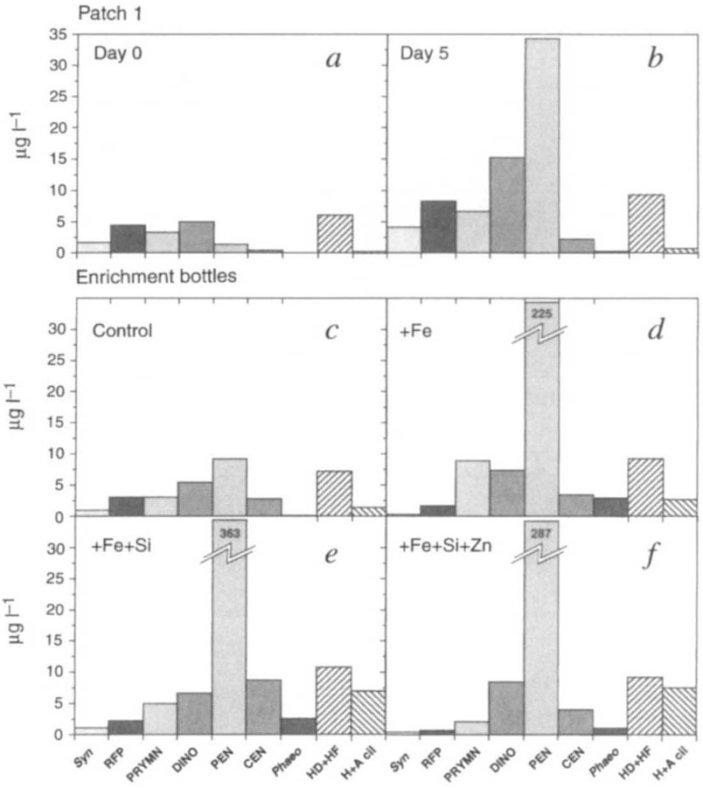

FIG. 4 *a*, Plankton community composition within patch 1 at day 0 of the experiment as expressed in μg C l^{-1}. This composition is similar to that observed at the 'outside-patch' stations over time. The groups represented include: *Syn*, *Synechococcus* spp.; RFP, red fluorescing picoplankton; PRYMN, Prymnesiophytes; DINO, autotrophic dinoflagellates; PEN, pennate diatoms; Phaeo, *Phaeocystis*; HD + HF, heterotrophic dinoflagellates + heterotrophic flagellates; H + A cil, heterotrophic+ autotrophic ciliates. Shaded bars indicate autotrophic biomass and diagonally hatched bars indicate heterotrophic biomass (the most likely grazers on the smaller size fraction of autotrophs). *b*, Taxonomic composition of patch 1 on day 5 of the experiment indicating increases in all classes of phytoplankton, especially the diatoms. *c*–*f*, Results of the bottle enrichment experiments performed on deck in 20-litre carboys[8] to test the effects of other potentially limiting nutrients. Water was collected using 30-litre Go Flo bottles deployed on Kevlar hydrowire and tripped with a Teflon messenger. Water was transferred to acid-cleaned, 20-litre polycarbonate bottles within a class 100 clean lab. chained to the deck of the ship. Treatments include: *c*, control, nothing added; *d*, +2 nM iron added; *e*, +2 nM iron, +10 μM silicic acid; *f*, +2 nM iron, +10 μM silicic acid, +2 nM zinc. Results indicate that diatoms in bottle enrichments with added iron outperformed the mesoscale experiment and that bottles with added silicic acid enhanced diatom growth relative to those without silicic acid. Zinc did not appear to have a positive effect on growth. Note the scale break in the diatom bar. Numbers at the top of the bar indicate the micrograms of carbon per unit volume attained in this group.

biomass can account for about 75% of the increase in POC. The remainder can be attributed to the accumulation of detrital carbon as dead plankton remains, as there is no appreciable terrigenous source in this area. DOC also increased, and the change accounted for about 25% of the overall increase in fixed carbon. Overall, there was a net accumulation of approximately 14 μM C in patch 1 on day 6. Oxygen concentrations within patch 1 show a 31 μM increase over initial stations. As exchange with the atmosphere would tend to reduce the oxygen anomaly, this value represents a minimum estimate of total new production during the experiment. Based on a Redfield carbon:oxygen ratio of 106:138, the corresponding estimate in terms of carbon is 24 μM C. Nitrate drawdown at this time was of the order of 4 μM, which corresponds to an organic carbon production of about 27 μM C. Similarly, the deficit in f_{CO_2} is equivalent to an increase in fixed organic carbon of 20 μM C.

The different estimates of carbon new production suggests that between 5 and 12 μM C was exported from the surface layer. The lack of larger mesozooplankton grazers, which commonly produce rapidly sinking faecal pellets that transport carbon below the mixed layer[35], suggest grazing export did not remove this missing carbon. Much of the missing carbon lost from the patch was probably removed by vertical mixing and possibly sinking of diatom aggregates. There was a 20-fold reduction in SF_6 concentration, of which only 60% can be accounted for by exchange with the atmosphere. The remainder of the SF_6, and much of the chemical and biological signal produced in the patch by iron enrichment, was eroded from the base of the mixed layer by exchange with waters moving relative to the advection of patch 1 and spread horizontally within the mixed layer.

Potential role of other nutrients

Shipboard bottle experiments (*in vitro* enrichments) were designed to test whether other factors such as zinc or silicate would reach such low concentrations that phytoplankton production would be limited after iron deficiency had been relieved. Zinc is required for both silicate uptake[36] and carbonic anhydrase activity, and it is depleted to subnanomolar concentrations in surface waters. Polycarbonate carboys (20-litre capacity) were filled with pre-enrichment water then augmented with the following treatments: [+0], [+2 nM Fe], [+2 nM Zn], [+10 μM Si], [+2 nM Fe, +2 nM Zn], [+2 nM Fe, +2 nM Zn, +10 μM Si]. The biological response in these *in vitro* experiments was monitored from sub-samples drawn from these carboys and analysed for a wide variety of parameters[7,10]. The results from the addition of 2 nM Zn and 10 μM Si (no added iron) were similar to the control (+0) and are not depicted here. The resultant taxanomic compositions are shown together with the patch 1 response in Fig. 4*b–e*. The results from the bottle experiments to which only iron was added were similar to those observed in patch 1. The treatments which included iron and silicate, both with and without zinc, may have slightly out-performed the treatment with iron but not containing silicic acid. This indicates that, following the relaxation of iron deficiency, supplemental amounts of silicate allow for greater diatom growth. There is some evidence to suggest that carbon uptake may be limited by carbonic anhydrase activity brought on by zinc deficiency[37] under bloom conditions where the concentration of CO_2 is low. Even at the picomolar concentrations of dissolved zinc detected (100 pM; R.M.G., unpublished results), our results (Fig. 4) are not consistent with zinc limitation in these waters, even when growth is stimulated by iron addition.

The species composition of the phytoplankton community that responds to iron addition can greatly influence the magnitude of the geochemical response. Our results indicate that iron enrichment favours diatoms. There are few natural instances where nitrate is in abundance and silicate is not. With few exceptions[38] therefore, silicate is not likely to limit carbon export. (We note that in the temperate North Atlantic Ocean, for example, seasonal blooms of diatoms may utilize nearly all the silicate, then sink out leaving residual nitrate and promoting the succession of other phytoplankton groups (ref. 38).) Given the short residence time of iron in the mixed layer, depletion of silicate will probably not occur in response to natural iron additions. It is likely that diatom growth will dominate the response to natural iron additions.

Comparison to natural systems

The two ecosystem-scale iron-enrichment experiments have produced large changes in biomass and ecosystem composition. The multiple iron additions in 1995 produced massive blooms and large drawdowns in CO_2 and nutrients. Resource utilization in these equatorial Pacific ecosystems is indeed controlled by iron availability[39]. The resultant drawdown of carbon dioxide in the surface waters of the fertilized patch provides for a sink (or in this case, an attenuated source) for atmospheric carbon dioxide[40]. These results, together with several recent studies[3,12,14,20,37,41], strongly support the hypothesis that iron transport to these, and other high nutrient areas, regulates carbon dioxide uptake and—at least if this occurs in the Southern Ocean—may directly influence global climate[40].

These experiments give us cause to consider how realistic these iron additions were, and if there are any natural analogues for these enrichments. Iron inputs of this magnitude are not uncommon in certain regions of today's oceans, or over wide regions of the ocean during the Last Glacial Maximum. If we assume that the input of iron during these experiments lasted about two weeks, then the flux of iron for both patch 1 and patch 3 was approximately 2 and 0.3 mmol m^{-2} yr^{-1} respectively. Present-day atmospheric iron fluxes to the nitrate-limited equatorial Atlantic are of the order of 2 mmol m^{-2} yr^{-1} (ref. 42). Fluxes of iron to the Pacific Ocean range from >2 mmol m^{-2} yr^{-1} east of Japan to 0.02 mmol m^{-2} yr^{-1} in the eastern equatorial Pacific[35]. Our observations in coastal systems with abundant nitrate suggest that most of the particulate iron can be solubilized by iron-starved plankton (K.S.J., unpublished data). If this is the case, the fluxes of iron in our experiments are only 10–100 times higher than the ambient flux in the equatorial Pacific and lie within the range of fluxes found in the North Pacific.

Fluxes of continental dust preserved in ice cores of Greenland and Antarctica indicate a 30-fold increase in dust flux during the Last Glacial Maximum[43]. Using isotopic tracers of export production, investigators have recently shown that there was increased ice-age carbon export to sediments of the Southern Ocean that was contemporaneous with increases of iron fluxes to these waters[41]. As indicated in the sediments downwind of Patagonia, the fluxes of iron to the glacial Southern Ocean increased by 5–10 times and were on the order of 5 mmol m^{-2} yr^{-1}. These rates of atmospheric iron delivery are similar to those used in the IronEx II experiment. Furthermore, the level of iron enrichment in patch 3 was designed to mimic the concentration of iron in the equatorial undercurrent at 140° W (ref. 23). It has been suggested that the shoaling or upwelling of this current is responsible for the increases in production along the equatorial Pacific[23]. These studies indicate that these enrichment experiments were comparable with natural iron fluxes and naturally induced iron concentrations. As such, we would expect dramatic increases in equatorial Pacific primary production to occur as a result of the increased iron flux during glacial times. Even if only 20% of the iron is soluble, a 50-fold change in iron flux would be comparable to the patch 3 (+0.3 nM Fe) experiment.

Conclusions

Mesoscale iron fertilization experiments demonstrate both the feasibility and utility of manipulative experiments in the open ocean. Through these experiments there now exists a preponderance of evidence in support of the 'iron hypothesis' (that iron availability limits phytoplankton growth and biomass in the HNLC regions of the world's oceans). As this working hypothesis has been given such strong support by both experimental and palaeoceanograhic observations, it is now time to regard the 'iron hypothesis' as the 'iron theory'. The natural corollary to this theory

is the suggestion that biological production in the ocean, stimulated by increased iron availability during the Last Glacial Maximum, was responsible for the observed low atmospheric levels of CO_2 (ref. 46). Such a corollary has found support in the observations of Kumar and co-workers[37] indicating increased export of carbon to sub-Antarctic sediments during the Last Glacial Maximum at times of higher iron flux. A present-day test of this corollary would have it's greatest significance in the Southern Ocean[40] where most of the HNLC waters are found and where the palaeoclimate coherence between iron flux and carbon export has been observed. Owing to extreme turbulence and temporal variability, a mesoscale enrichment experiment in these Southern Ocean waters poses a tantalizing, yet formidable, challenge. □

Received 8 May; accepted 5 September 1996.

1. Chisolm, S. W. & Morel, F. M. M. (eds) *Limnol. Oceanogr.* **36,** 1507–1964 (1991).
2. Siegenthaler, U. in *The Role of Air-Sea Exchange in Geochemical Cycling* (ed. Buat-Menard, P.) 209–247 (Reidel, Boston, 1986).
3. Price, N. M., Anderson, L. F. & Morel, F. M. M. *Deep-Sea Res.* **38,** 1361–1378 (1991).
4. Landry, M. R. *et al. Limnol. Oceanogr.* (in the press).
5. Martin, J. H., Gordon, R. M., Fitzwater, S. E. & Broenkow, W. W. *Deep-Sea Res.* **36,** 649–680 (1989).
6. Martin, J. H., Fitzwater, S. E. & Gordon, R. M. *Glob. Biogeochem. Cycles* **4,** 5–12 (1990).
7. Martin, J. H., Gordon, R. M. & Fitzwater, S. E. *Limnol. Oceanogr.* **36,** 1793–1802 (1991).
8. Coale, K. H. *Limnol. Oceanogr.* **36,** 1851–1864 (1991).
9. De Baar, H. J. W. *et al. Mar. Ecol. Prog. Ser.* **65,** 34–44 (1990).
10. Price, N. M., Ahner, B. A. & Morel, F. M. M. *Limnol. Oceanogr.* **39,** 520–534 (1994).
11. Johnson, K. S., Coale, K. H., Elrod, V. E. & Tindale, N. W. *Mar. Chem.* **46,** 319–334 (1994).
12. Fitzwater, S. E., Coale, K. H., Gordon, R. M., Johnson, K. S. & Ondrusek, M. E. *Deep-Sea Res. II* **43** (in the press).
13. Banse, K. *Limnol. Oceanogr.* **35,** 772–775 (1990).
14. Dugdale, R. C. & Wilderson, F. P. *Glob. Biogeochem. Cycles* **4,** 13–19 (1990).
15. Frost, B. W. *Limnol. Oceanogr.* **36,** 1616–1630 (1991).
16. Martin, J. H. *et al. Nature* **371,** 123–129 (1994).
17. Watson, A. J. *et al. Nature* **371,** 143–145 (1994).
18. Johnson, K. S., Gordon, R. M., Coale, K. H. & Elrod, V. A. Eos **76,** OS154 (1996).
19. Banse, K. *Nature* **375,** 112 (1995).
20. Bruland, K. W., Donat, J. H. & Hutchins, D. H. *Limnol. Oceanogr.* **36,** 1555–1577 (1991).
21. Zhuang, G. & Duce, R. A. *Deep-Sea Res.* **40,** 1413–1429 (1993).
22. Csanady, G. T. in *Ocean Dumping of Industrial Wastes* (eds Ketchum, B. H., Kester, D. R. & Park, P. K. D.) 109–129 (Plenum, New York, 1978).
23. Coale, K. W., Fitzwater, S. E., Gordon, R. M., Johnson, K. S. & Barber, R. T. *Nature* **379,** 621–624 (1996).
24. Dugdale, R. C. & Goering, J. J. *Limnol. Oceanogr.* **12,** 196–206 (1967).
25. Sanderson, M. P., Hunter, C. N., Fitzwater, S. E., Gordon, R. M. & Barber, R. T. *Deep-Sea Res.* **42,** 431–440 (1995).
26. Chavez, F. P. *et al. Limnol. Oceanogr.* **36,** 1816–1833 (1991).
27. Booth, B. C. *Bot. Mar.* **30,** 101–108 (1987).
28. Landry, M. R., Kirshtein, J. & Constantiniou, J. *Mar. Ecol. Prog. Ser.* **120,** 53–63 (1995).
29. Chavez, F. P. *Glob. Biogeochem. Cycles* **3,** 27–35 (1989).
30. Chavez, F. P. & Smith, S. S. in *Upwelling in the Ocean: Modern Processes and Ancient Records* (eds Summerhayes, C. P., Emeis, K. C., Angel, M. V., Smith, R. L. & Zeitzschel, B.) 149–169 (Wiley, Chichester, 1995).
31. Chavez, F. P., Buck, K. R., Service, S. K., Newton, J. & Barber, R. T. *Deep-Sea Res.* (in the press).
32. Latasa, M., Landry, M. R., Schluter, L. & Bidigare, R. R. *Limnol. Oceanogr.* (in the press).
33. Fasham, M. J. R. *Deep-Sea Res.* **42,** 1111–1149 (1995).
34. Huntley, M. E. & Lopez, M. D. G. *Am. Nat.* **140,** 210–242 (1992).
35. Paffenhofer, G. A. & Knowles, S. C. *J. Mar. Res. II* **37,** 35–49 (1979).
36. Rueter, J. G. & Morel, F. M. M. *Limnol. Oceanogr.* **26,** 67–73 (1981).
37. Morel, F. M. M. *et al. Nature* **369,** 740–742 (1994).
38. Milliman, J. D. (ed.) *Deep-Sea Res. II* **40,** (1993).
39. Behrenfeld, M. J. *et al. Nature* **383,** 508–511 (1996).
40. Cooper, D. J., Watson, A. J. & Nightingale, P. D. *Nature* **383,** 511–513 (1996).
41. Kumar, N. *et al. Nature* **378,** 675–680 (1995).
42. Duce, R. A. & Tindale, N. W. *Limnol. Oceanogr.* **36,** 1715–1726 (1991).
43. Yung, Y. L., Lee, T., Wang, C. H. & Shieh, Y. T. *Science* **271,** 962–963 (1996).
44. Obata, H., Karatani, H. & Nakayama, E. *Anal. Chem.* **65,** 1524–1528 (1994).
45. Bruland, K. W., Franks, R. P., Knauer, G. A. & Martin, J. H. *Anal. Chim. Acta* **155,** 233–245 (1979).
46. Martin, J. H. *Paleoceanography* **5,** 1–13 (1990).

ACKNOWLEDGEMENTS. We thank the crew and officers of the RV *Melville* for their assistance at sea; our co-workers and colleagues at Moss Landing Marine Laboratories for their assistance; A. Longhurst for comments that greatly improved this manuscript; and the many scientists, both funded and unfunded, who contributed their resources and talents to this project. It is to this spirit of unselfish collaboration that we owe much of our success and our heartfelt thanks. This work was supported in part by the US National Science Foundation, the US Office of Naval Research, the Monterey Bay Aquarium Research Institute, the Centro de Investigacion Cientifica y Education Superior de Ensenada, and the UK Natural Environment Research Council.

CORRESPONDENCE should be addressed to K.H.C. (e-mail: coale@mlml.calstate.edu).